IJICTR
International Journal of Information & Communication Technology Research

Volume 15- Number 2 – 2023 (1 -11)

Transmitted Data Security in Non-Orthogonal Multiple Access Networks with Directional Modulation Based on User Location

Sepahdar Falsafi
Faculty of Electrical and Computer Engineering
Imam Hossain Comprehensive University
Tehran, Iran
Falsaf1389@gmail.com

Hamidreza Khodadadi*
Faculty of Electrical and Computer Engineering
Imam Hossain Comprehensive University
Tehran, Iran
fajr@ihu.ac.ir

Received: 25 July 2022 – Revised: 11 December 2022 - Accepted: 23 January 2023

Abstract—**In Non-orthogonal multiple access, a user with a weaker channel gain is assigned more power than a user with a stronger channel. This type of power allocation allows the strong user (SU) to apply the successive interference cancellation (SIC) method that first detects the symbols of the weak user (WU) before detecting its data. The SIC method makes the WU data vulnerable to eavesdropping at the SU and so increases the detection complexity. This paper studies the physical layer security of the data against eavesdropping. The proposed scheme uses directional modulation that distorts the symbols transmitted in an undesired direction therefore the external eavesdroppers receive different symbols. It becomes complicated for an external eavesdropper to track and detect the signal of legitimate users. This scheme eliminates the WU data on the location of the SU so the strong user does not need the SIC. We analyze the impacts of various factors on security, such as the number of antennas and the secrecy rate.**

Keywords: component, NOMA, directional modulation, DM-RFDA, eavesdropper, secrecy.

Article type: Research Article

Publisher: ICT Research Institute

[DOI: 10.61186/itrc.15.2.1]

I. INTRODUCTION

NOMA has attracted the attention of many researchers to the 5G and future wireless communications in recent years. This technology provides fairness in resource allocation and spectral efficiency and increases the number of customers. NOMA exploits the power domain based on the channels' gain to generate superimposed signals at the transmitter and use successive interference cancellation (SIC) at the receiver side. A user with a weaker channel quality is allocated more power than a user with a stronger one. This type of power allocation allows the strong user (SU) to perform SIC, which first detects the symbols of the weak user (WU). Using the SIC by SU makes the WU data vulnerable to eavesdropping at the SU and increases the complexity detection at SU [1-3]. Directional modulation (DM), employed in physical layer security for wireless communication, preserves the constellation of the confidential message along a predefined direction while disturbing the constellation

* Corresponding Author

of the confidential message in other directions [4]. The difference between the DM and conventional beamforming is in the way of producing the array weights. In conventional beamforming, array weights only depend on the transmission direction of the desired receiver, but in DM, the array weights depend on the direction and the data symbol rate. Therefore, the low probability of interception (LPI) and low probability of detection (LPD) can be obtained.

In [5] and [6], the DM was constructed using a phased antenna array. This type (DM-PA) exploits individual array element excitation reconfigurability. In [7-8], a robust DM algorithm by calculation errors is presented. This method uses DM technology on the baseband by using beamforming and artificial noise (AN). The DM constructed by PA only is angle-dependent. When the eavesdropper (Eve) is located along the legitimate user (LU) direction, it can receive and demodulate the signal transmitted for LU. A linear frequency diverse array (LFDA) in [9-10] proposed a new method for DM to solve the PA problem and obligate a secure transmission where the LU and Eve have the same direction but a different distance from the transmitter. In other words, the DM-LFDA produces a radiation pattern controlled by direction and range. However, in [10], the direction and range achieved by LFDA are coupled. This couple means the eavesdropper may have multiple direction-range pairs to receive the same signals as LU. To address the problem of LFDA, the authors in [11-15] propose a random frequency diversity array (RFDA) model. In this method, the frequency increments are determined randomly for all antenna-array elements. Using DM-RFDA, confidential messages can be securely and precisely transmitted to a given location. RFDA can decouple the correlation between the direction and range. This means that RFDA can solve the problem of LFDA. In [1], a DM technology is presented to protect the WU data from a SU in the NOMA network. This scheme conceals the WU data from SU by distorting them at the SU.

In this paper, signals transmitted for SU and WU do not have a crossover by obtaining the receiver's position and applying the DM technology. For this reason, SU does not need the SIC to detect WU data and eliminate them. With no need for the SIC, the detection complexity for SU is reduced.

The remainder of this paper is outlined as follows. In Section II, we review the basics of RFDA-DM. Next, we introduce the system model in section III. In Section IV, we analyze the security of the system model, test results, and discussion. Finally, concluding remarks and future work are given in Section V.

Notations: I_N and $[\cdot]^H$ denote the N×N identity matrix. Signs $[\cdot]^H$, $[\cdot]^{-\dagger}$, $[\cdot]^{-1}$ denote complex conjugate transpose (Hermitian), Moore-Penrose pseudo-inverse and inverse, respectively. Operation $\|\cdot\|$ denotes the norm of a complex number. Throughout the paper, matrices, vectors, and scalars are denoted by letters of bold upper case, bold lower case, and lower case, respectively.

II. BASICS OF RFDA-DM

The frequency increment method between the antenna elements in RFDA is different from the LFDA. Like Fig. 1, the frequency assigned to antenna number one up to the central antenna of the array is equal to:

$$f_n = f_c + k_n \Delta f \ , \quad n = 0,1,\cdots,(N-1)/2 \tag{1}$$

The frequency assigned to antenna number $(N-1)$ up to $(N+1)/2$ is equal to the frequency allocated to antenna number one up to number $(N-3)/2$, respectively that given by

$$f_m = f_n, m = (N-1),\cdots,(N+1)/2 \ , n = 0,\cdots,(N-3)/2 \tag{2}$$

We consider a uniform linear array (ULA) and the phase reference set at the array geometric center, f_c is the central carrier frequency and Δf is the frequency increment. All the k_n are independent and identically distributed (i.i.d.) random variables. k_n, determines a random mapping rule to determine the carrier frequencies for the different elements, and R_n is the distance of the receiver to the n-th elements. The distance between the receiver and antenna array is far, thus R_n can be approximated as

$$R_n = R - b_n d\cos(\theta) \ , \quad n = 0,1,2,\cdots,N-1 \tag{3}$$

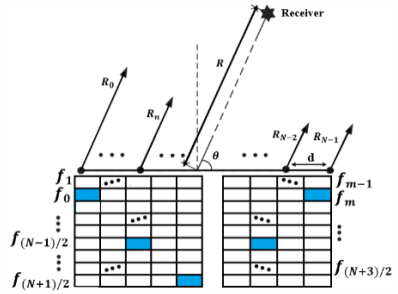

Figure 1. RFDA Array Structure

In equation (3), θ and R are the angle and distance between LU to the centre of the transmitter array, respectively, and d is the element spacing in the ULA. b_n is given by

$$b_n = n - \frac{N-1}{2} \tag{4}$$

For simplicity, the normalized line-of-sight (LOS) channel in free space is considered throughout this paper. Thus, for an arbitrary user located at (R,θ), the normalized steering vector based on the RFDA is equal to

$$\mathbf{h}(\mathbf{R},\boldsymbol{\theta}) = \frac{1}{\sqrt{N}}\left[e^{j\psi_0(R,\theta)},\cdots,e^{j\psi_{N-1}(R,\theta)}\right]^T \tag{5}$$

The signal phase of the reference element at the location of the receiver is equal to:

$$\phi_0(R,\theta) = 2 f_c \frac{\pi R}{c} \tag{6}$$

The signal phase of the n-th element at the location of the receiver is equal to:

[DOI: 10.61186/itrc.15.2.1]

$$\phi_n(R,\theta)=2f_n\frac{\pi R_n}{c}=2(f_c+k_n\Delta f)\frac{\pi R_n}{c}$$
$$=2\left(f_c\frac{\pi R}{c}-b_n\frac{f_c d\pi\cos(\theta)}{c}+k_n\Delta f\frac{\pi R}{c}-b_n k_n\frac{\Delta f d\pi\cos(\theta)}{c}\right) \quad (7)$$

The third expression in (7) shows that the radiation pattern depends on the distance and the frequency increment, which is important for this reason. We know that $N\Delta f \le f_c$ and we suppose that element spacing d is equal to $\lambda/2$. The fourth expression in (7) is too small and ignorable. Thus, the phase shift for each antenna element can be approximated by [11]

$$\psi_n(R,\theta)=\phi_n(R,\theta)-\phi_0(R,\theta)$$
$$=2\left(-b_n\frac{\pi\cos\theta}{2}+k_n\Delta f\frac{\pi R}{c}\right) \quad (8)$$

Putting equation (8) in (5), the radiation pattern will be a function of R and θ.

III. SYSTEM MODEL

This paper investigates the PLS security in the single-cell downlink with Power Domain NOMA-based (PD-NOMA). The transmitter has two LUs and uses the same frequency for them. The transmitter knows the locations of LUs and can simultaneously send two beams for them. The LUs and Eve have single antennas. The synthesis of the system is described in Fig. 2. (R_1,θ_1) and (R_2,θ_2) $\{where\ \theta_1,\theta_2\in[0^\circ \quad 180^\circ];R_1,R_2\in[0.5km \quad 5.5km]\}$ belonged to SU and WU locations, respectively.

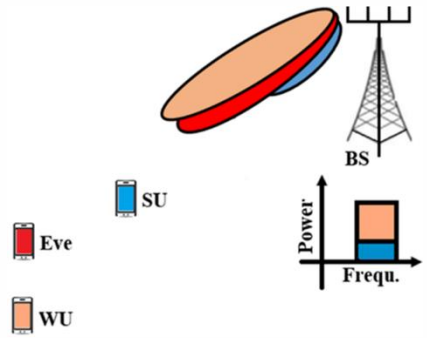

Figure 2. Proposed downlink NOMA

We want to prevent eavesdropping and interception of WU data by Eve and SU and also reduce the detection complexity at SU. The channel vectors for SU and WU are given by $\mathbf{h_1}$ and $\mathbf{h_2}$, respectively, where $\|\mathbf{h}_1\|\ge\|\mathbf{h}_2\|$.

$$\mathbf{h_1}=\sqrt{\frac{1}{N}}\left[e^{j\psi_0(R_1,\theta_1)},e^{j\psi_1(R_1,\theta_1)},\cdots,e^{j\psi_{N-1}(R_1,\theta_1)}\right]^T \quad (9)$$

$$\mathbf{h_2}=\sqrt{\frac{1}{N}}\left[e^{j\psi_0(R_2,\theta_2)},e^{j\psi_1(R_2,\theta_2)},\cdots,e^{j\psi_{N-1}(R_2,\theta_2)}\right]^T \quad (10)$$

To simplify the expression, the steering vectors of LUs can compose a steering matrix as follows

$$\mathbf{H}=[\mathbf{h}_1 \quad \mathbf{h}_2] \quad (11)$$

P is the total power of the transmitter. s_i and w_i are independent information data streams that are transmitted for SU and WU respectively. Each of them has QPSK modulation [16] and we assume that $\|s_i\|=\|w_i\|=1$. β_3 and $\mathbf{g_3}$ are the power allocation factor (PAF) and the beamforming vector for random artificial noise (RAN), respectively. RAN is sent in all directions but it is perpendicular to the channel vector of the LUs.

The PAF for SU and WU are given by β_1 and β_2, respectively where $\beta_1\le\beta_2$. We assigned the most power to the weaker user. The minimum power for RAN is equal to the power assigned to WU; so the power of RAN is greater than the power of information signals in any places, making it difficult for Eve, to detect the information signals. In other words, $\beta_2\le\beta_3$ And the PAF for users are equal to:

$$\beta_1=\frac{2P\|\mathbf{h}_2\|^2}{2(\|\mathbf{h}_1\|^2+2\|\mathbf{h_2}\|^2)} \quad (12)$$

$$\beta_2=\frac{P(\|\mathbf{h}_1\|^2+\|\mathbf{h_2}\|^2)}{2(\|\mathbf{h}_1\|^2+2\|\mathbf{h_2}\|^2)} \quad (13)$$

The PAF for RAN is equal to:

$$\beta_3=\frac{P(\|\mathbf{h}_1\|^2+\|\mathbf{h_2}\|^2)}{2(\|\mathbf{h}_1\|^2+2\|\mathbf{h_2}\|^2)} \quad (14)$$

The PAF satisfies the below condition

$$\beta_1+\beta_2+\beta_3=P \quad (15)$$

$\mathbf{g_1}$ and $\mathbf{g_2}$ are the array excitation or beamforming vectors for SU and WU respectively [16-17]

$$\mathbf{g_1}=\frac{\left[\mathbf{I_N}-\left(\mathbf{h_2^H}\right)^\dagger\mathbf{h_2^H}\right]\mathbf{h_1}}{\left\|\left[\mathbf{I_N}-\left(\mathbf{h_2^H}\right)^\dagger\mathbf{h_2^H}\right]\mathbf{h_1}\right\|^2} \quad (16)$$

$$\mathbf{g_2}=\frac{\left[\mathbf{I_N}-\left(\mathbf{h_1^H}\right)^\dagger\mathbf{h_1^H}\right]\mathbf{h_2}}{\left\|\left[\mathbf{I_N}-\left(\mathbf{h_1^H}\right)^\dagger\mathbf{h_1^H}\right]\mathbf{h_2}\right\|^2} \quad (17)$$

The property of equations (16) and (17) is that $\mathbf{h_1^H}\cdot\mathbf{g}_2=0$ and $\mathbf{h_2^H}\cdot\mathbf{g}_1=0$. The data streams and RAN have the same symbol rate. As shown in Fig. 3, the transmitted superposition coding (SC) signal for the SU and WU is equal to

$$\mathbf{g_i}=[\mathbf{g}_1\ \mathbf{g}_2]\begin{bmatrix}\sqrt{\beta_1}s_i\\ \sqrt{\beta_2}w_i\end{bmatrix}+\sqrt{\beta_3}\mathbf{g_3}z_i \quad (18)$$

$\mathbf{z}$ is an N-tuple vector with the probability density function (PDF) being $CN(0,I_N)$, called RAN, and defined as follows

$$\mathbf{g}_3=\mathbf{I}_N-\mathbf{H}(\mathbf{H}^H\mathbf{H})^{-1}\mathbf{H}^H \quad (19)$$

[DOI: 10.61186/itrc.15.2.1]

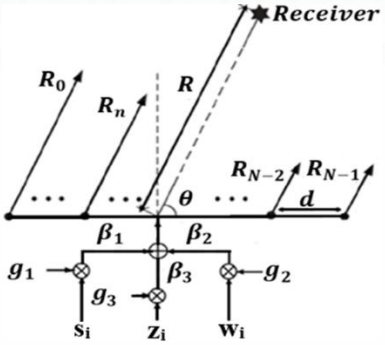

Figure 3. Array Excitations

According to equation (19), we know that $\mathbf{g_3}$ is perpendicular to $\mathbf{H}^H$. Thus, RAN does not affect the SU and WU. So the received signal at the SU is equal to:

$$y_1 = \mathbf{h_1^H g}_i + n_1 = \sqrt{\beta_1}\mathbf{h_1^H g_1} s_i + n_1 \quad (20)$$

The inter-cluster interference (ICI) and RAN are eliminated due to the type of design (i.e., $\mathbf{h_1^H} \cdot \mathbf{g}_2 = 0$, $\mathbf{h}_1^H \cdot \mathbf{g}_3 = 0$). According to equation (20), the SU does not need the SIC for detection. In the same way, the received signal at the WU is equal to:

$$y_2 = \mathbf{h_2^H g}_i + n_2 = \sqrt{\beta_2}\mathbf{h_2^H g}_2 w_i + n_2 \quad (21)$$

The received signal at Eve is equal to:

$$\begin{aligned} y_e &= \mathbf{h^H g_i} + n_e \\ &= \mathbf{h^H}\sqrt{\beta_1}\mathbf{g_1} s_i + \mathbf{h^H}\sqrt{\beta_2}\mathbf{g_2} w_i + \sqrt{\beta_3}\mathbf{h^H g_3} z_i + n_e \end{aligned} \quad (22)$$

n_1 , n_2 *and* n_e are the AWGN with the zero mean and variances σ_1^2 , σ_2^2 and σ_e^2 , respectively.

IV. Performance Analysis

In this section, we will simulate the constellation diagram, signal amplitude, signal phase, security rate (SR), BER, and SINR performance of our proposed method. Detailed parameters in the simulations are listed in Table I.

TABLE I. List of Simulation Parameters

Parameter	Value
Modulation mode	QPSK
Number of ULA antennas, N	15
Central frequency, f_c	1 GHz
Δf	1MHz
Total transmit power, P	1
Number of LUs	2
Number of unknown eavesdroppers	1
Location of SU, $(\mathbf{R_1}, \boldsymbol{\theta_1})$	$(2500, 45^\circ)$
Location of WU $(\mathbf{R}_2, \boldsymbol{\theta}_2)$	$(4500, 45^\circ)$
Location of an unknown eavesdropper	All places
Power of AWGN, $\sigma_1^2 = \sigma_2^2 = \sigma_e^2$	0.1

A. Time and Space Complexity

Regardless of the number of random frequencies f_n for all methods, the computational complexity of the Max SLNR-based approach [8], the orthogonal vector approach (OV) [16], and the proposed method are analyzed. In the OV approach, the power pattern along the desired directions (for 2 LUs) must be obtained first and the orthogonal basis in the null space of H must be generated. The principal operation of the proposed approach is the calculation of $\mathbf{g}_1$ (or $\mathbf{g}_2$) and $\mathbf{g}_3$. The computational complexity of the Max-SLNR-based approach, the OV approach, and the proposed approach are shown in Table II, where Null (0) represents the operation of obtaining the orthogonal basis in the null space of a matrix and Eig (0) represents the operation of obtaining the eigenvector corresponding to the largest eigenvalue of a square matrix. As shown in table II, the proposed approach has the lowest computational complexity.

The sizes of the orthogonal matrix and the AN z can impact the memory consumption significantly. As shown in Table II, the size of the orthogonal matrix for the proposed method is N × N. and the size of the inserted AN z for all methods is N× 1.

TABLE II. Computational Complexity of DM

Approaches	Major Operation	Complexity of calculation
Max SLNR-based [8]	$X_1 = \iint_{\Omega_e} hh^H d\theta + \frac{\sigma_w^2}{\beta_1^2 P}\mathrm{I}_N$ $\mathrm{X}_2 = (X_1)^{-1}\mathrm{HH}^H$ $X_3 = Eig(X_2)$ $x_4 = \mathbf{I}_N - (\mathbf{H}^H)^\dagger \mathbf{H}^H$	$O(LN^2)$ $O(N^3)$ $O(N^3)$ $O(2N^2)$
OV [16]	$y_1 = Null(\mathbf{H}^H)$ $y_2 = s_1\Lambda_1 + w_1\Lambda_2$	$O(N^3)$ $O(2N^2)$
[1]	$x^{(m)} = x_1 + x_2$ $x_1 = \sqrt{P_1}\frac{\mathbf{h}_1}{\|\mathbf{h}_1\|}(a^{(m)} - \frac{\|\mu\|^2 \delta^{(i,m)}}{1-\|\mu\|^2})$ $x_2 = \sqrt{P_2}\frac{\mathbf{h}_2}{\|\mathbf{h}_2\|}(a_2 - \sqrt{\frac{P_1}{P_2}}\frac{\mu\delta^{(i,m)}}{1-\|\mu\|^2})$ $\mu = \frac{\mathbf{h}_2^H \mathbf{h}_1}{\|\mathbf{h}_2\|\|\mathbf{h}_1\|}$ $\delta^{(i,m)} = \frac{1}{L}\sum_{a^{(m)} \in A^{(i)}} a^{(m)} - a^{(m)}$ $c^{(i)} = \frac{1}{L}\sum_{a^{(m)} \in A^{(i)}} a^{(m)}$	$O \succ 4N^3$
Proposed	$\mathbf{g}_1 = \left[\mathbf{I_N} - \left(\mathbf{h_2^H}\right)^\dagger \mathbf{h_2^H}\right]\mathbf{h_1}$ $\mathbf{g}_3 = \mathbf{I}_N - \mathbf{H}(\mathbf{H}^H\mathbf{H})^{-1}\mathbf{H}^H$	$O(2N^2)$ $O(2N^2)$

[DOI: 10.61186/itrc.15.2.1]

B. Reception BER

Analytical closed-form BER expressions were derived for the SU and WU in appendix A. By using the closed-forms (equations (23) and (24)) we compare the analytical and simulation BER in the proposed DM system.

$$P_{s,SU}^{I} = Q\left(\sqrt{\frac{2}{\sigma_2^2}}d_1\right) + 0.5Q\left(\sqrt{\frac{2}{\sigma_2^2}}d'_2\right) \quad (23)$$

$$P_{s,WU} = 1-\left(1-P_{s,SU}^{I}\right)^2 = 1-\left(1-P_{s,SU}^{Q}\right)^2 \quad (24)$$

Fig. 4. shows the performance of BER versus SNR for SUs and WUs. As shown in this Figure, it is noted that the BER performance of the proposed method is much better than the method in [1] as the SNR increases.

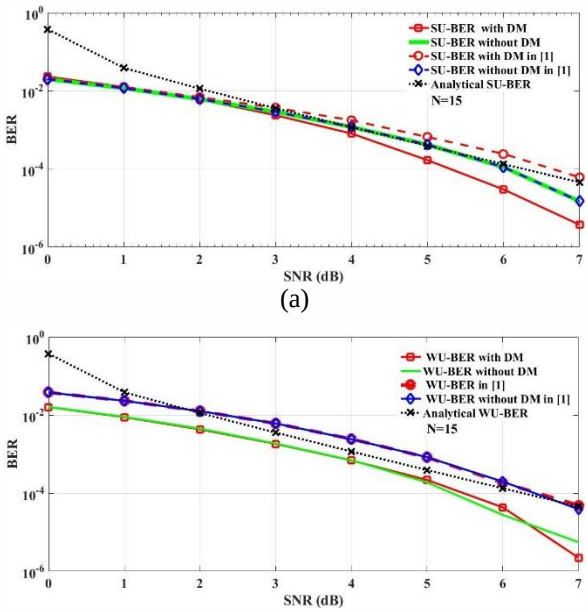

Figure 4. The performance of BER versus SNR: (a) For SUs, (b) For WUs

Fig. 5 shows the performance of BER versus the number of antenna for SUs and WUs. As shown in this Figure, it is noted that the BER performance is much better as the number of antenna elements increases, and the proposed method is much better than the method in [1].

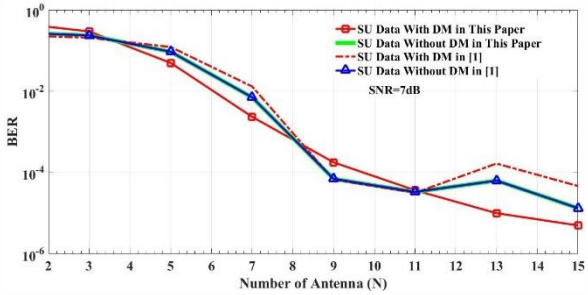

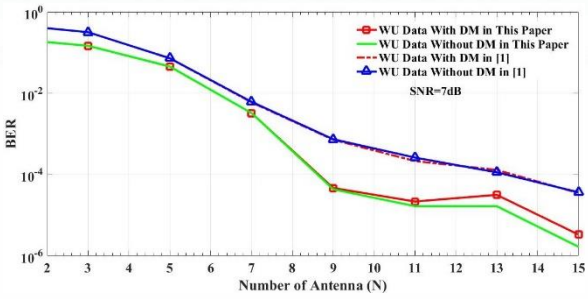

Figure 5. The performance of BER versus the number of antenna: (a) For SUs, (b) For WUs

Since BER is a receiver functionality dependent we assumed a standard receiver that decodes received noisy symbols based on which quadrant the constellation points locate into. The BER performance of the proposed DM system with the standard QPSK receiver is depicted in Fig. 6. It can be seen that BER is very low at the location of LU and WU, and very high in another location.

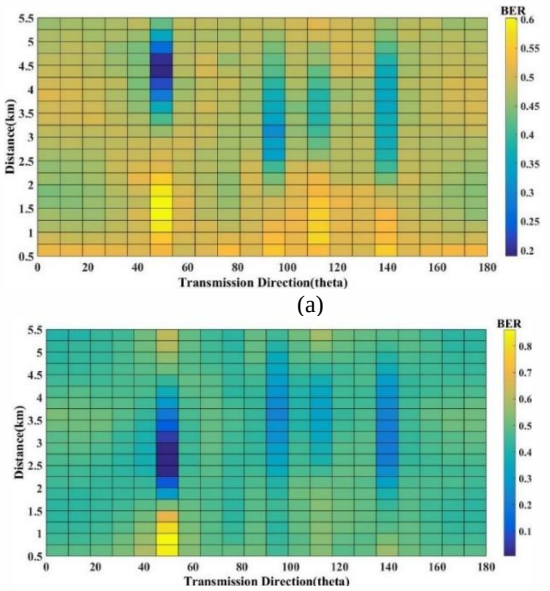

Figure 6. BER versus any location: (a) For WU signal, (b) For SU signal

As shown in Fig. 4, 5, and 6, the proposed system with DM and without DM has almost the same BER in the location of LUs. This is the DM capability that only distorts the symbols at the Eves location and increases the BER for them.

C. Constellation

For transmission 16 symbols 11, the constellation signal at SU and Eve locations are shown in Fig.7. It is noted that "11" in the text is the binary equivalent of decimal 3. This simulation shows that the SU receives all symbols correctly (shown in dark circle marker) but Eve (We assume that it is in the location $(3500, 45^{\circ})$) receives only one symbol correctly (shown in red pentagram marker).

[DOI: 10.61186/itrc.15.2.1]

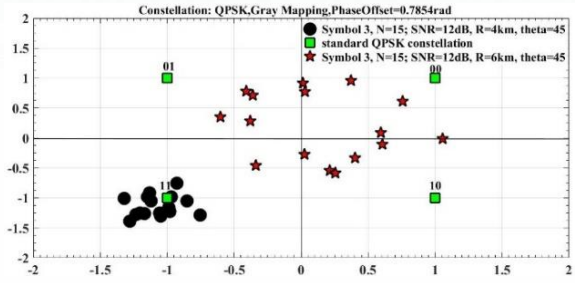

Figure 7. Constellation of 16 symbols 11 in SU and Eve

Fig. 8 shows that the amplitudes and the phases of the transmitted signals versus distance. For 2000 QPSK symbols transmitted, the simulation shows that the amplitudes of all transmitted signals (shown in different colors) pass through one point at the location of LUs. In other words, all signals have the same amplitude at the location of LUs but different amplitudes at other locations. Also, in the location of LUs, all signals have standard QPSK phases, but in another places, they have different and non-standard QPSK phases.

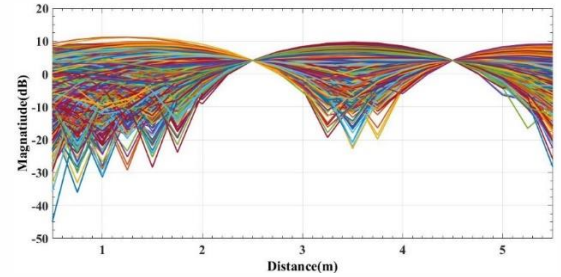

(a)

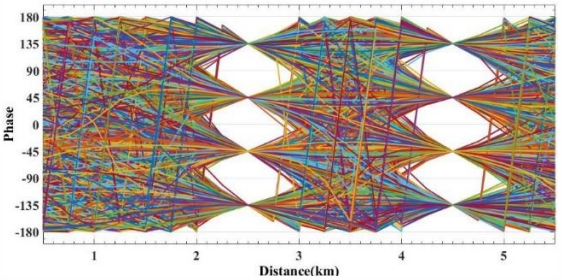

(b)

Figure 8. Receive signal at SU and WU: (a) amplitudes, (b) Phases.

D. Secrecy rate for unknown eavesdroppers' *location*

The secrecy rate (SR) of information for SU (s_i signal) is given by [18]

$$R_s = \left[R(R_1,\theta_1) - R(R_e,\theta_e) \right]^+ \tag{25}$$

$$R(R_1,\theta_1) = \log_2\left(1+\frac{\left\|\sqrt{\beta_1}\mathbf{h}_1^{\mathbf{H}}\mathbf{g}_1 s_i\right\|^2}{\sigma_1^2}\right) \tag{26}$$

$$R(R_e,\theta_e) = \log_2\left(1+\frac{\left\|\sqrt{\beta_1}\mathbf{h}^{\mathbf{H}}\mathbf{g}_1 s_i\right\|^2}{\left\|\sqrt{\beta_1}\mathbf{h}^{\mathbf{H}}\mathbf{g}_2 w_i\right\|^2+\left\|\sqrt{\beta_3}\mathbf{h}^{\mathbf{H}}\mathbf{g}_3 z_i\right\|^2+\sigma_e^2}\right) \tag{27}$$

So the SR is equal to

$$R_s = \left[R(R_1,\theta_1) - R(R_e,\theta_e) \right]^+ \tag{28}$$

The SR w_i is calculated similarly. According to Equations (26) and (27), if $\boldsymbol{h}^{\boldsymbol{H}}(\boldsymbol{R},\boldsymbol{\theta}) = \boldsymbol{h}_1^{\boldsymbol{H}}(\boldsymbol{R}_1,\boldsymbol{\theta}_1)$ then $\left\|\sqrt{\beta_1}\mathbf{h}^{\mathbf{H}}\mathbf{g}_2 w_i\right\|^2$ and $\left\|\sqrt{\beta_3}\mathbf{h}^{\mathbf{H}}\mathbf{g}_3 z_i\right\|^2$ equal to zero and R_s will be the lowest value. Based on equation (29), no more than one point scarifies this condition.

$$\psi_n(R,\theta) = 2\left(-b_n\frac{\pi cos\theta_1}{2}+k_n\Delta f\frac{\pi R_1}{c}\right) \tag{29}$$

As shown in Fig. 9 and Fig. 10 the direction and distance achieved by the RFDA are uncoupled. Uncouple distance and direction mean that there are no points where Eve can receive the confidential signal as LUs.

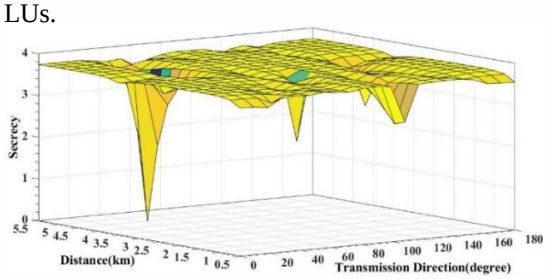

(a)

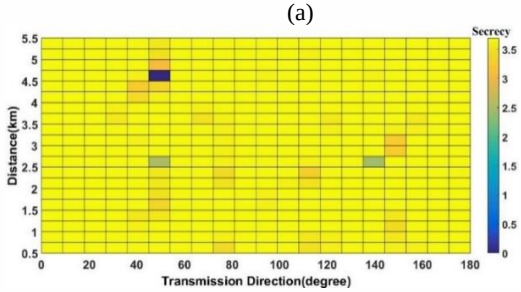

(b)

Figure 9. Secrecy rate for WU: (a) Three-Dimensional, (b) Two-Dimensional.

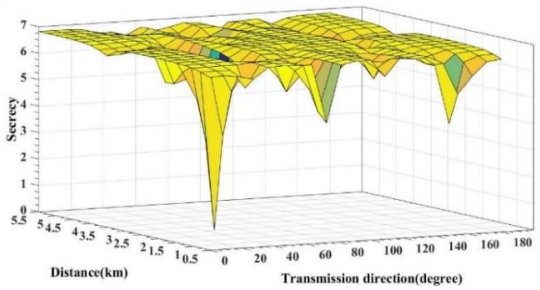

(a)

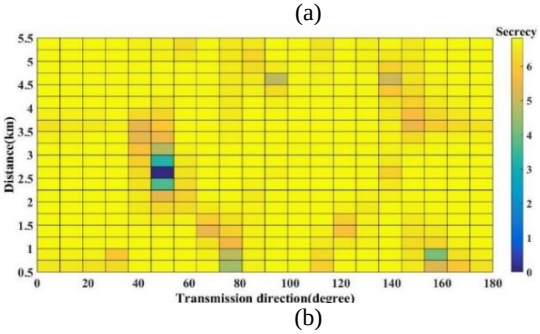

(b)

Figure 10. Secrecy rate for SU: (a) Three-Dimensional, (b) Two-Dimensional.

With an increase the number of array elements, the SR for LUs will be increased but as shown in Fig. 11,

[DOI: 10.61186/itrc.15.2.1]

the SR in the proposed method is better than to reference [1].

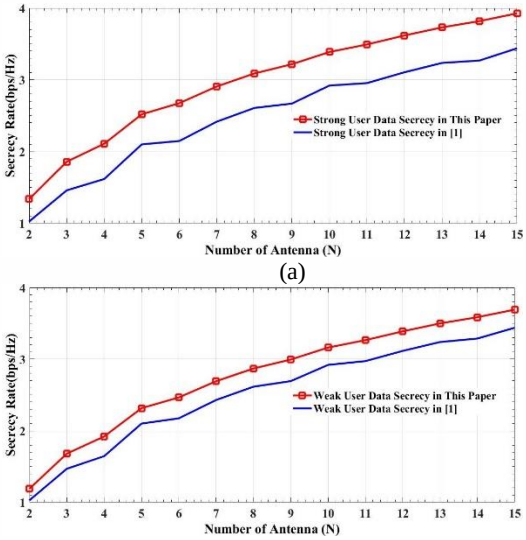

Figure 11. The performance of SR versus the number of antenna: (a) For SUs, (b) For WUs

E. SINR value in different locations

The SINR *value* for different locations is equal to:

$$SINR = \frac{\left\|\sqrt{\beta_1}\mathbf{h}^{\mathbf{H}}\mathbf{g}_1 s_i\right\|^2}{\left\|\sqrt{\beta_1}\mathbf{h}^{\mathbf{H}}\mathbf{g}_2 w_i\right\|^2 + \left\|\sqrt{\beta_3}\mathbf{h}^{\mathbf{H}}\mathbf{g}_3 z_i\right\|^2 + \sigma_e^2} \quad (30)$$

The simulation of SINR is shown in Fig. 12 and Fig. 13. It is clear that in the places where $\boldsymbol{h}^{\boldsymbol{H}}(R,\theta)$ is equal to $\boldsymbol{h}_1^{\boldsymbol{H}}(R_1,\theta_1)$, the SINR has highest value.

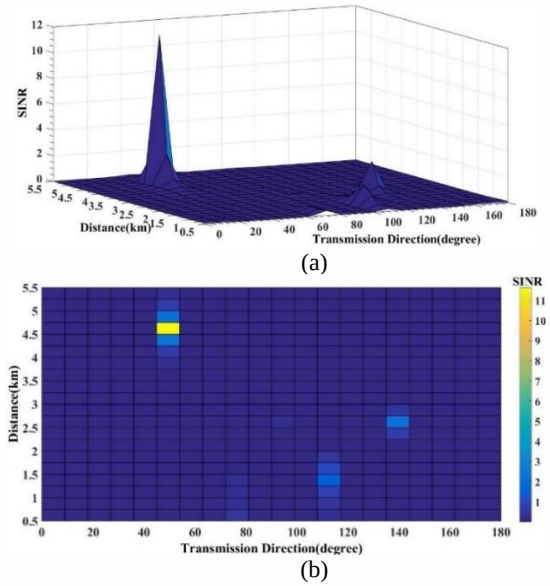

Figure 12. SINR for WU: (a) Three-Dimensional, (b) Two-Dimensional

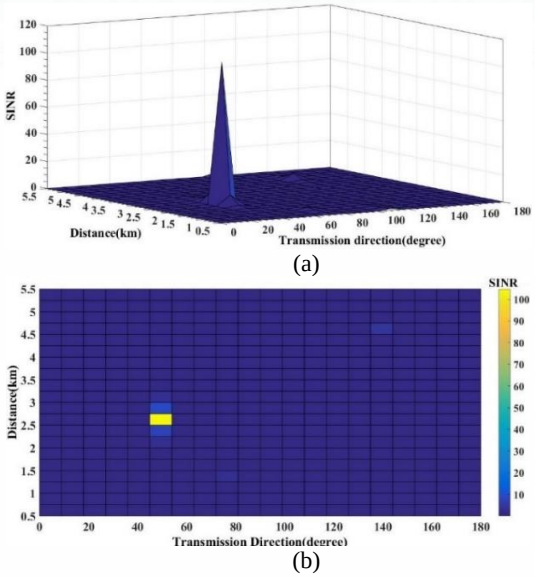

Figure 13. SINR for SU: (a) Three-Dimensional, (b) Two-Dimensional.

V. ESTIMATION ANGLE ERROR

Appendix B presents the estimation of angle error, and a synthesis method based on conditional MMSE was proposed to calculate the estimation error. The excitation signal vector and RAN vector were developed according to the probability distribution of the angle error. The received signal with the error angle along the WU direction is:

$$\begin{aligned} y_2(\hat{\theta}_2) &= \boldsymbol{h}_2^{\boldsymbol{H}}(\hat{\theta}_2)\hat{\mathbf{g}}_i + n_2 \\ &= \sqrt{\beta_1}\boldsymbol{h}_2^{\boldsymbol{H}}(\hat{\theta}_2)\mathbf{R}_4 s_i + \sqrt{\beta_2}\boldsymbol{h}_2^{\boldsymbol{H}}(\hat{\theta}_2)(\mathbf{R} + \frac{1}{\gamma}\mathbf{I}_N)^{-1}\mathbf{B}w_i \\ &+ \sqrt{\beta_3}\boldsymbol{h}_2^{\boldsymbol{H}}(\hat{\theta}_2)(\mathbf{I}_N - \mathbf{R})z_i + n_2 \end{aligned} \quad (31)$$

Fig. 14 shows the BER performance at a specified $\Delta\theta_m = 7^\circ$ and the SNR is set to 7 dB, respectively. In the desired direction, it shows that the BER performance of the method with an imperfect angle is better than the method with a perfect angle. However, Eve can intercept the transmitted useful symbols of imperfect angles easier than the case of perfect angles because of the wide main lobe.

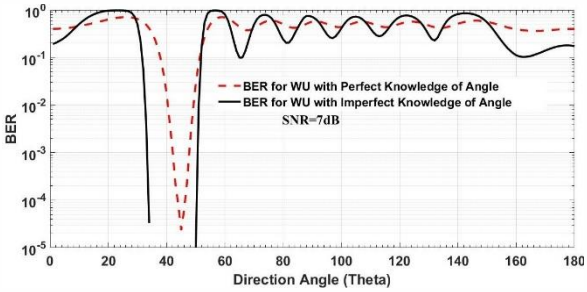

Figure 14. The performance of BER versus direction angle

The distance error is equal to $\Delta R = R\tan(\Delta\theta_m)$, based on the main lobe antenna radiation pattern. In a practical system, the direction of angle is usually obtained by some classic estimation algorithms such as MUSIC or GPS which measurement error or $\Delta\theta_m$ of them is less than seven degree.

[DOI: 10.61186/itrc.15.2.1]

VI. CONCLUSION

This paper presents DM technology based on RFDA to protect the WU data from the SU and vice versa in wireless communications. The DM-RFDA secures the data transmission in angle and range. In reference [1], SU receives WU data but with distorted modulation. In this paper, not only the signals are distorted in undesired locations, but also they are orthogonal to each other. In other words, two steering vectors for construct DM ($\mathbf{g}_1$ and $\mathbf{g}_2$) are orthogonal to each other along their prescribed locations. This orthogonality means two information data streams can be conveyed along their selected locations without crossover. As a result, the WU data and SU data are protected from each other and Eve. Eve receives the distortion constellation. Simulation affirmation that 1) This method can significantly outperform the SR and sum rate compared to [1], 2) with increasing the number of array elements, the BER for LUs decreases, 3) In Reference [1], SU needs the SIC to remove WU data, but this proposed method does not need SIC because WU data is eliminated on the SU and vice versa (without crossover). With no need for the SIC, the detection complexity is reduced for SU, 4) A RFDA established security for data transmission when the LU and Eve locate in a different location. The reference [1] creates security only in the angle, but in this method, the confidential messages can be securely and precisely transmitted to a given location. This method was proposed to be applied to satellites, unmanned aerial vehicles, millimeter-wave networks, and so on. For fairness between the LUs, the power distribution in this scheme needs to be improved.

REFERENCES

[1] R. M. Christopher and D. K. Borah, "Physical Layer Security for Weak User in MISO NOMA Using Directional Modulation (NOMAD)," IEEE Commun. Lett., vol. 24, no. 5, pp. 956–960, 2020.

[2] M. A. Ahmed, A. Baz, and C. C. Tsimenidis, "Performance analysis of NOMA systems over Rayleigh fading channels with successive interference cancellation," IET Commun., vol. 14, no. 6, pp. 1065–1072, 2020.

[3] W. U., Khan, Z., Yu, S., Yu, G. A. S., Sidhu, & J., Liu, "Efficient power allocation in downlink multi-cell multi-user NOMA networks," IET Communications, vol.13, no. 4, pp.396-402, 2019.

[4] Y. Ding and V. Fusco, "A review of directional modulation technology," Int. J. Microw. Wirel. Technol., vol. 8, no. 7, pp. 981–993, 2016.

[5] A. H. Chang, A. Babakhani, and A. Hajimiri, "Near-field direct antenna modulation (NFDAM) transmitter at 2.4GHz," IEEE Antennas Propag. Soc. AP-S Int. Symp., pp. 2–5, 2009.

[6] M. P. Daly and J. T. Bernhard, "Directional modulation technique for phased arrays," IEEE Trans. Antennas Propag., vol. 57, no. 9, pp. 2633–2640, 2009.

[7] J. Hu, F. Shu, and J. Li, "Robust Synthesis Method for Secure Directional Modulation with Imperfect Direction Angle," IEEE Commun. Lett., vol. 20, no. 6, pp. 1084–1087, 2016.

[8] F. Shu, X. Wu, J. Li, R. Chen, and B. Vucetic, "Robust synthesis scheme for secure multi-beam directional modulation in broadcasting systems," IEEE Access, vol. 4, pp. 6614–6623, 2016.

[9] J. Xiong, S. Y. Nusenu, and W. Q. Wang, "Directional Modulation Using Frequency Diverse Array For Secure Communications," Wirel. Pers. Commun., vol. 95, no. 3, pp. 2679–2689, 2017.

[10] P. F. Sammartino, C. J. Baker, and H. D. Griffiths, "Frequency diverse MIMO techniques for radar," IEEE Trans. Aerosp. Electron. Syst., vol. 49, no. 1, pp. 201–222, 2013.

[11] J. Hu, S. Yan, F. Shu, J. Wang, J. Li, and Y. Zhang, "Artificial-Noise-Aided Secure Transmission with Directional Modulation Based on Random Frequency Diverse Arrays," IEEE Access, vol. 5, pp. 1658–1667, 2017.

[12] Y. Liu, H. Ruan, L. Wang, and A. Nehorai, "The Random Frequency Diverse Array: A New Antenna Structure for Uncoupled Direction-Range Indication in Active Sensing," IEEE J. Sel. Top. Signal Process., vol. 11, no. 2, pp. 295–308, 2017.

[13] J. Gao, Z. Yuan, B. Qiu, and J. Zhou, "Secure Multi users Directional Modulation Scheme Based on Random Frequency Diverse Arrays in Broadcasting Systems," Secure. Commun. Networks, vol. 2020, 2020.

[14] S. Wang, S. Yan, J. Zhang, N. Yang, R. Chen, and F. Shu, "Secrecy Zone Achieved by Directional Modulation with Random Frequency Diverse Array," IEEE Trans. Veh. Technol., vol. 70, no. 2, pp. 2001–2006, 2021.

[15] J. Xie, B. Qiu, Q. Wang, and J. Qu, "Broadcasting directional modulation based on random frequency diverse array," Wirel. Commun. Mob. Comput., vol. 2019, 2019.

[16] Y. Ding and V. Fusco, "Orthogonal vector approach for the synthesis of multi-beam directional modulation transmitters," IEEE Antennas Wirel. Propag. Lett., vol. 14, no. March, pp. 1330–1333, 2015.

[17] Y. Ding and V. F. Fusco, "Directional modulation far-field pattern separation synthesis approach," IET Microwaves, Antennas Propag., vol. 9, no. 1, pp. 41–48, 2015.

[18] M. Hafez, M. Yusuf, T. Khattab, T. Elfouly, and H. Arslan, "Secure Spatial Multiple Access Using Directional Modulation," IEEE Trans. Wirel. Commun., vol. 17, no. 1, pp. 563–573, 2018.

[19] Cejudo, E. C., Zhu, H., & Alluhaibi, "On the power allocation and constellation selection in downlink NOMA. IEEE 86th Vehicular Technology Conference (VTC-Fall) (pp. 1-5). IEEE, 2017.

APPENDIX A

DERIVATION OF ANALYTICAL BER FOR NOMA

With a SU (LU1) and a WU (LU2) in the downlink NOMA scenario, the transmitter transmits a SC signal $x = \sqrt{\beta_1 P}\mathbf{g}_1 x_1' + \sqrt{\beta_2 P}\mathbf{g}_3 x_2' = x_1 + x_2$, x_i' is the symbol to user i from a signal constellation χ_i, and the super-symbol x belongs to the superposed constellation χ. The PAF β_i determines the location of the super-constellation points. For any two superposed constellations χ_i of size M_i ($i \in \{1,2\}$), the size of χ equal to $\prod_i M_i$ under direct superposition mapping. The received signal at LU is $y_i = \mathbf{h}_i x + n_i$. By assigning a greater power to the WU, interference from SU's signal x_1 is small and WU is able to decode its own signal x_2 without perform SIC. SU is able to decode x_2 since $\|P_2\| \geq \|P_1\|$ and removes this interference and then decodes its own signal x_1.

Fig. 15 represents the constellations for SU and WU BPSK+BPSK-modulated signals. The resulting super-constellation is formed by 4 super-symbols. WU's decision regions are each of the 2 states, whereas for SU there are 4 different decision regions.

To determine a given constellation's decoding error probability (EP), we consider the layout and number of

[DOI: 10.61186/itrc.15.2.1]

constellation points and the minimum Euclidean distance (d_{min}) among them. The EP of WU is conditioned by the incoming interference from SU's signal, which can either reduce or increase WU's d_{min} . SU uses a SIC, so an error in decoding WU's symbol means that the decoding of SU's signal is also unsuccessful, due to error propagation. Hence, the achievable symbol error probability (P_s) of SU is affected by WU's transmit symbols. Assuming that P_s in decoding is caused by incoming interference from the nearest neighbor. In this scenario, the bit error probability equal to $P_b = P_S / log_2^{M_i}$ [19].

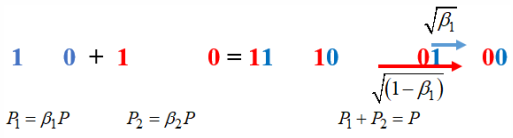

Figure 15. NOMA superposed two BPSK constellation

E_{bi} refers to the average bit energy of LUi before superposition. Fig.16 represents the result of the superposition two BPSK constellations in the NOMA method. The resulting super-constellation is formed by four symbols of different amplitude in one dimension only. The set of distances between each pair of points is given by

$$d_1 = \sqrt{\beta_1 E_{b1}} \tag{32}$$

$$d_2 = \sqrt{\beta_2 E_{b2}} = \sqrt{(1-\beta_1) E_{b2}} \tag{33}$$

$$d'_2 = d_2 - d_1 = \left\| \sqrt{\beta_2} h_2^H g_2 \right\|^2 - \left\| \sqrt{\beta_1} h_1^H g_1 \right\|^2 \tag{34}$$

Where d_2 and d_1 are the distances between points in WU's layer (red points in Fig. 16) and SU's layer, respectively.

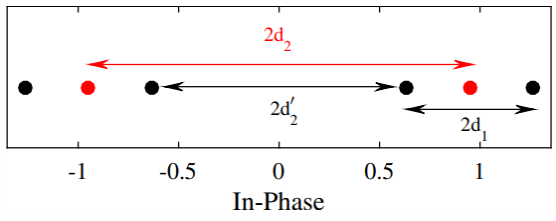

Figure 16. d_{min} Constellation [19]

The super-constellation for QPSK+QPSK is symmetrical in both dimensions, and equations (32)-(34) apply to the I and Q components, which have the same error probability.

WU's P_S : $P_{S,WU}$ is that of a QPSK-constellation affected by interference from SU's symbols in both the in-phase and quadrature dimensions. In the worst case, when the transmit NOMA symbol is adjacent to the imaginary axis, the EP is equivalent to that of a QPSK constellation with $d_{min,WU} = 2d_2^{'}$. In the best case, when the NOMA constellation points are furthest from the origin, $d_{min,WU} = 2(d'_2 + 2d_1)$. The average of P_S for each situation yields the following expression:

$$P_{s,WU}^I = \frac{1}{2}\left[Q\left(\sqrt{\frac{2}{\sigma_2^2}} d'_2 \right) + Q\left(\sqrt{\frac{2}{\sigma_2^2}} (d'_2 + 2d_1) \right) \right] \tag{35}$$

Due to I/Q symmetry, the joint P_S results:

$$P_{S,WU} = 1 - \left(1 - P_{S,WU}^I\right)^2 = 1 - \left(1 - P_{S,WU}^Q\right)^2 \tag{36}$$

SU's P_S : The super-constellation in this case is made up of 16 non-equidistant symbols. On each dimension, there are 2 types of constellation points: 2 outer points, with the nearest neighbor located at a distance $2d_1$; and 2 inner points, with two adjacent points located at distances $2d_1$ and $2d'_2$, respectively. Thus, the error probability is [19]

$$P_{s,SU}^I = Q\left(\sqrt{\frac{2}{\sigma_2^2}} d_1 \right) + 0.5Q\left(\sqrt{\frac{2}{\sigma_2^2}} d'_2 \right) \tag{37}$$

As the EP on each dimension is identical, the joint P_S can be calculated by substituting (35) into

$$P_{s,WU} = 1 - \left(1 - P_{s,SU}^I\right)^2 = 1 - \left(1 - P_{s,SU}^Q\right)^2 \tag{38}$$

APPENDIX B

DERIVATION OF LOCATION ERROR

Generally, the transmitter needs to know the value of the location of the desired user in advance. For simplicity, we only calculate the estimation of the angle. In a practical system, the direction of departure (DoD) is usually obtained by some classic estimation algorithms such as GPS or MUSIC. However, a small error in the DoD estimation will cause an angle mismatch between the steering vector and the excitation vector which degrade the performance of the DM system. To address this problem, we will recalculate the excitation vector, denoted by $\hat{\mathbf{g}}_1$, $\hat{\mathbf{g}}_2$, and $\hat{\mathbf{g}}_3$, for combating the estimation errors of the direction angles. Due to the estimation error, we have $\hat{\theta}_i = \theta_i + \Delta\theta_i$, where $\Delta\theta_i$ is the angle error and $\hat{\theta}_i$ is the estimated angle. we assume $\Delta\theta_i$ is uniformly distributed over the interval $[-\Delta\theta_m \quad \Delta\theta_m]$. Note that $\Delta\theta_m$ represents the maximum angle error and it is a positive value up to the beam width between first nulls which is equal to $\Delta\theta_m = 4/N$ Radians. The distance error is equal to $\Delta R = R\tan(\Delta\theta_i)$, which in this article, its calculations are omitted). $p(\Delta\theta_i)$ denote the probability distribution of $\Delta\theta_i$. We have [7]

$$p(\Delta\theta_i) = \begin{cases} \dfrac{1}{2\Delta\theta_m} & \Delta\theta_m \le \Delta\theta_i \le \Delta\theta_m \\ 0 & others \end{cases} \tag{39}$$

For simplicity, we only calculate the estimation of the WU angle, so g_3 can be considered as follows which is perpendicular to the $\mathbf{h}_2$

[DOI: 10.61186/itrc.15.2.1]

$$\mathbf{g}_3 = \left[\mathbf{I_N} - \mathbf{h}_2\mathbf{h}_2^{\mathbf{H}}\right] \tag{40}$$

The expectation of the $\hat{g}_3$ matrix to $\hat{\theta}_2$ equal to:

$$E_{\hat{\theta}_2}[\hat{g}_3(\hat{\theta}_2)] = E_{\hat{\theta}_2}\left[\mathbf{I_N} - [\mathbf{h}_2(\theta_2+\Delta\theta_2)\mathbf{h}_2^{\mathbf{H}}(\theta_2+\Delta\theta_2)\right]$$
$$= \mathbf{I_N} - \underbrace{E_{\hat{\theta}_2}[\mathbf{h}_2(\theta_2+\Delta\theta_2)\mathbf{h}_2^{\mathbf{H}}(\theta_2+\Delta\theta_2)]}_{\mathbf{R}} = \mathbf{R}_2 \tag{41}$$

The expectation of the $\hat{g}_2$ matrix to $\hat{\theta}_1$ and $\hat{\theta}_2$ equal to:

$$\hat{g}_2 = E_{\hat{\theta}_1}(E_{\hat{\theta}_2}(\left[\mathbf{I_N} - \left(\mathbf{h}_1^{\mathbf{H}}\right)^{-1}\mathbf{h}_1^{\mathbf{H}}\right]\mathbf{h}_2))$$
$$= E_{\hat{\theta}_2}(\mathbf{I_N}\mathbf{h}_2) - E_{\hat{\theta}_1}(\left(\mathbf{h}_1^{\mathbf{H}}\right)^{-1}\mathbf{h}_1^{\mathbf{H}})E_{\hat{\theta}_2}(\mathbf{h}_2)$$
$$= \mathbf{I_N}\underbrace{E_{\hat{\theta}_2}(\mathbf{h}_2)}_{B} - \underbrace{E_{\hat{\theta}_1}(\left(\mathbf{h}_1^{\mathbf{H}}\right)^{-1}\mathbf{h}_1^{\mathbf{H}})}_{A}\underbrace{E_{\hat{\theta}_2}(\mathbf{h}_2)}_{B} = \mathbf{R}_3 \tag{42}$$

The expectation of the $\hat{g}_1$ matrix to $\hat{\theta}_1$ and $\hat{\theta}_2$ equal to:

$$\hat{g}_1 = E_{\hat{\theta}_2}(E_{\hat{\theta}_1}(\left[\mathbf{I_N} - \left(\mathbf{h}_2^{\mathbf{H}}\right)^{-1}\mathbf{h}_2^{\mathbf{H}}\right]\mathbf{h}_1))$$
$$= E_{\hat{\theta}_1}(\mathbf{I_N}\mathbf{h}_1) - E_{\hat{\theta}_2}(\left(\mathbf{h}_2^{\mathbf{H}}\right)^{-1}\mathbf{h}_2^{\mathbf{H}})E_{\hat{\theta}_1}(\mathbf{h}_1)$$
$$= \mathbf{I_N}\underbrace{E_{\hat{\theta}_1}(\mathbf{h}_1)}_{C} - \underbrace{E_{\hat{\theta}_2}(\left(\mathbf{h}_2^{\mathbf{H}}\right)^{-1}\mathbf{h}_2^{\mathbf{H}})}_{D}\underbrace{E_{\hat{\theta}_1}(\mathbf{h}_1)}_{C} = \mathbf{R}_4 \tag{43}$$

The **A** is calculated through computing expectation to $\hat{\theta}_i$, in which the entry at the m-th row and the n-th column is computed as follows

$$A_{mn} = \int_{-\Delta\theta_m}^{\Delta\theta_m} e^{2\pi j(m-n)\cos(\theta_1+\Delta\theta_1)}p(\Delta\theta_1)d(\Delta\theta_1)$$
$$= \int_{-\Delta\theta_m}^{\Delta\theta_m}\frac{1}{2\Delta\theta_m}(e^{2\pi j(m-n)\cos(\theta_1+\Delta\theta_1)})d(\Delta\theta_1)$$
$$= \int_{-\Delta\theta_m}^{\Delta\theta_m}\frac{1}{2\Delta\theta_m}(e^{2\pi j(m-n)(\cos(\theta_1)\cos(\Delta\theta_1)-\sin(\theta_1)\sin(\Delta\theta_1))})d(\Delta\theta_1) \tag{44}$$

In order to simplify Eq. (44), let

$$a_{mn} = j2\pi(m-n)\cos(\theta_1)$$
$$b_{mn} = -j2\pi(m-n)\sin(\theta_1) \tag{45}$$

Substituting Eq. (45) in Eq. (44) yields

$$A_{mn} = \int_{-\Delta\theta_m}^{\Delta\theta_m}\frac{1}{2N\Delta\theta_m}(e^{(a_{mn}\cos(\Delta\theta_1)+b_{mn}\sin(\Delta\theta_1))})d(\Delta\theta_1) \tag{46}$$

In the same way

$$R_{mn} = \int_{-\Delta\theta_m}^{\Delta\theta_m}\frac{1}{2\Delta\theta_m}(e^{(a_{mn}\cos(\Delta\theta_2)+b_{mn}\sin(\Delta\theta_2))})d(\Delta\theta_2) \tag{47}$$

The column vector **B** is calculated through computing expectation to $\hat{\theta}_i$ as follows

$$B_{n1} = \int_{-\Delta\theta_m}^{\Delta\theta_m} e^{\pi j(n-\frac{(N+1)}{2})\cos(\theta_2+\Delta\theta_2)}p(\Delta\theta_2)d(\Delta\theta_2)$$
$$= \int_{-\Delta\theta_m}^{\Delta\theta_m}\frac{1}{2\Delta\theta_m}(e^{\pi j(n-\frac{(N+1)}{2})\cos(\theta_2+\Delta\theta_2)})d(\Delta\theta_2)$$
$$= \int_{-\Delta\theta_m}^{\Delta\theta_m}\frac{1}{2\Delta\theta_m}(e^{\pi j(n-\frac{(N+1)}{2})(\cos(\theta_2)\cos(\Delta\theta_2)-\sin(\theta_2)\sin(\Delta\theta_2))})d(\Delta\theta_2) \tag{48}$$

In order to simplify Eq. (48), let

$$c_n = \pi j(n-\frac{(N+1)}{2})\cos(\theta_2)$$
$$f_n = -\pi j(n-\frac{(N+1)}{2})\sin(\theta_2) \tag{49}$$

Substituting Eq. (49) in Eq. (48) yields

$$B_{n1} = \int_{-\Delta\theta_m}^{\Delta\theta_m}\frac{1}{2\Delta\theta_m}(e^{(c_n\cos(\Delta\theta_2)+f_n\sin(\Delta\theta_2))})d(\Delta\theta_2) \tag{50}$$

The transmitted signal and received signal in Eq. (19) and (21) can be rewritten, respectively, as:

$$\hat{\mathbf{g}}_\mathbf{i} = \sqrt{\beta_1}\hat{\mathbf{g}}_\mathbf{1}s_i + \sqrt{\beta_2}\hat{\mathbf{g}}_2 w_i + \sqrt{\beta_3}E_{\hat{\theta}_2}[\mathbf{g}_3(\hat{\theta}_2)]z_i \tag{51}$$

$$y_2(\hat{\theta}_2) = \boldsymbol{h}_2^{\boldsymbol{H}}(\hat{\theta}_2)\hat{\mathbf{g}}_i + n_2$$
$$= \sqrt{\beta_1}\boldsymbol{h}_2^{\boldsymbol{H}}(\hat{\theta}_2)\hat{\mathbf{g}}_\mathbf{1}s_i + \sqrt{\beta_2}\boldsymbol{h}_2^{\boldsymbol{H}}(\hat{\theta}_2)\hat{\mathbf{g}}_2 w_i$$
$$+\sqrt{\beta_3}\boldsymbol{h}_2^{\boldsymbol{H}}(\hat{\theta}_2)\hat{\mathbf{g}}_\mathbf{3}z_i + n_2 \tag{52}$$

We will optimize the $\hat{g}_2$ vector based on the MMSE. The optimization problem can be formulated as:

$$\min E_{\hat{\theta}_2}\left[\left\|y_2(\hat{\theta}_2) - \sqrt{\beta_2}w_i\right\|^2\right] \tag{53}$$
$$s.t \quad \hat{\mathbf{g}}_2^H\hat{\mathbf{g}}_2 \le 1$$

The optimal solution of $\hat{g}_2$ is expressed as:

$$E_{\hat{\theta}_2}\left[\left\|y_2(\hat{\theta}_2) - \sqrt{\beta_2}w_i\right\|^2\right] = E_{\hat{\theta}_2}\left[\left\|\mathbf{h}_2^H(\hat{\theta}_2)\hat{\mathbf{g}}_i - \sqrt{\beta_2}w_i\right\|^2\right] + E\left\{n_2^H n_2\right\}$$
$$= E_{\hat{\theta}_2}\left[\left\|\sqrt{\beta_2}\mathbf{h}_2^H(\hat{\theta}_2)\hat{\mathbf{g}}_2 w_i - \sqrt{\beta_2}w_i\right\|^2\right] + \sigma^2\hat{\mathbf{g}}_2^H\hat{\mathbf{g}}_2$$
$$= E_{\hat{\theta}_2}\left[(\sqrt{\beta_2}\mathbf{h}_2^H(\hat{\theta}_2)\hat{\mathbf{g}}_2 w_i - \sqrt{\beta_2}w_i)^H(\sqrt{\beta_2}\mathbf{h}_2^H(\hat{\theta}_2)\hat{\mathbf{g}}_2 w_i - \sqrt{\beta_2}w_i\right]$$
$$+\sigma^2\hat{\mathbf{g}}_2^H\hat{\mathbf{g}}_2$$
$$= E_{\hat{\theta}_2}\left[\beta_2\hat{\mathbf{g}}_2^H\mathbf{h}_2(\hat{\theta}_2)\mathbf{h}_2^H(\hat{\theta}_2)\hat{\mathbf{g}}_2 - \beta_2\hat{\mathbf{g}}_2^H(\hat{\theta}_2)\mathbf{h}_2(\hat{\theta}_2) - \beta_2\mathbf{h}_2^H(\hat{\theta}_2)\hat{\mathbf{g}}_2 + \beta_2\right]$$
$$+\sigma^2\hat{\mathbf{g}}_2^H\hat{\mathbf{g}}_2 \tag{54}$$

We use $f(\hat{\mathbf{g}}_2)$ to represent the objective function of the optimization problem Eq. (54).

$$f(\hat{\mathbf{g}}_2) = \beta_2\hat{\mathbf{g}}_2^H\mathbf{R}\hat{\mathbf{g}}_2 - \beta_2\hat{\mathbf{g}}_2^H(\hat{\theta}_2)\mathbf{B} - \beta_2\mathbf{B}^H\hat{\mathbf{g}}_2 + \beta_2$$
$$+\sigma^2\hat{\mathbf{g}}_2^H\hat{\mathbf{g}}_2 \tag{55}$$

To obtain the optimal excitation vector, we need to compute the derivative of $f(\hat{\mathbf{g}}_2)$ to $\hat{g}_2$

$$\frac{\partial f(\hat{\mathbf{g}}_2)}{\hat{\mathbf{g}}_2} = 2\beta_2\mathbf{R}\hat{\mathbf{g}}_2 - 2\beta_2\mathbf{B} + 2\sigma^2\hat{\mathbf{g}}_2 \tag{56}$$

[DOI: 10.61186/itrc.15.2.1]

If $\frac{\partial f(\hat{\mathbf{g}}_2)}{\hat{\mathbf{g}}_2} = 0$, we obtain

$$\hat{\mathbf{g}}_2 = \beta_2(\beta_2\mathbf{R} + \sigma^2\mathbf{I}_N)^{-1}\mathbf{B} = (\mathbf{R} + \frac{\sigma^2}{\beta_2}\mathbf{I}_N)^{-1}\mathbf{B}$$

$$= (\mathbf{R} + \frac{1}{\gamma}\mathbf{I}_N)^{-1}\mathbf{B} \quad (57)$$

where $\gamma = \frac{\beta_2}{\sigma^2}$ is the SNR in the desired direction. The received signal along the WU direction is

$$y_2(\hat{\theta}_2) = \boldsymbol{h}_2^{\boldsymbol{H}}(\hat{\theta}_2)\hat{\mathbf{g}}_i + n_2$$

$$= \sqrt{\beta_1}\boldsymbol{h}_2^{\boldsymbol{H}}(\hat{\theta}_2)\mathbf{R}_4 s_i + \sqrt{\beta_2}\boldsymbol{h}_2^{\boldsymbol{H}}(\hat{\theta}_2)(\mathbf{R} + \frac{1}{\gamma}\mathbf{I}_N)^{-1}\mathbf{B}w_i$$

$$+\sqrt{\beta_3}\boldsymbol{h}_2^{\boldsymbol{H}}(\hat{\theta}_2)(\mathbf{I}_N - \mathbf{R})z_i + n_2 \quad (58)$$

Sepahdar Falsafi received his B.Sc. degree in Communication Engineering, in 2005 and the M.Sc. degree in 2015. He is a Ph.D. student of Communication Engineering at Imam Hossain Comprehensive University. His research interests include Wireless Communication Systems.

Hamid Reza Khodadadi received his Ph.D. degree in Imam Hossain Comprehensive University in the field of Communication Systems. He is an Associate Professor at Imam Hossain Comprehensive University Tehran, Iran. His research interests include Wireless Communication Systems, Free Space Optical Communication (FSO), Channel Coding, and Physical Layer Security

[DOI: 10.61186/itrc.15.2.1]